Excitation-energy dependence of the fission-fragment neutron-excess ratio

H. Paşca
Joint Institute for Nuclear Research, 141980 Dubna, Russia
and "Babeş-Bolyai" University, Faculty of Physics, 400084 Cluj-Napoca, Romania

A. V. Andreev,[1] G. G. Adamian,[1] and N. V. Antonenko[1,2]
[1]*Joint Institute for Nuclear Research, 141980 Dubna, Russia*
[2]*Tomsk Polytechnic University, 634050 Tomsk, Russia*

(Received 12 November 2022; revised 4 January 2023; accepted 25 January 2023; published 9 February 2023)

Within the improved scission-point fission model, it is shown that the average neutron number per proton is not the same in fission fragments and is not equal to that in a fissioning nucleus. For the induced fission of ^{238}U, ^{240}Pu, ^{244}Cm, and ^{250}Cf, the dependencies of the fission-fragment neutron-excess ratio on the shell structure and excitation energy of fragment are studied.

DOI: 10.1103/PhysRevC.107.024603

I. INTRODUCTION

Nuclear fission is a complex process, which involves the motion of the system in several relevant collective coordinates, such as the mass/charge asymmetry, deformation of the fission fragments, and the relative distance between the corresponding fragments. Therefore, the study of fission process is rather cumbersome, as one needs to take into account the changes of the potential energy, which drives the process, in all these collective coordinates. Because any change in the potential energy (driving potential) in any coordinate has large consequences on the observables, a good description of the driving potential is essential. The main problem lies in the fact that the driving potential can not be accessed directly from an experimental point of view. Thus, we have to rely on the measurements of the mass and charge distributions (the isotopic distribution of the fission fragments), the total kinetic energy (the deformation of the fission fragments), and neutron multiplicities (the excitation energy of the fission fragments), and then to extract the driving potential.

The driving potential is very sensitive to the mass-to-charge ratio of the fission fragments. For the induced fission of ^{234,235,238}U, ^{237,238}Np, ^{240}Pu, ^{244}Cm, and ^{250}Cf, the neutron-excess ratios, defined as the average neutron number per proton, i.e., $\langle N_{L,H}\rangle/Z_{L,H}$ ($\langle N_{L,H}\rangle$ is the average neutron number of the primary fission fragment with the charge number $Z_{L,H}$), have been studied by several groups in recent years [1–4]. As shown in Refs. [1–4], the measured neutron-excess ratios are not constant and governed by the shell effects. The mass-to-charge ratio of the fission fragments has been recently addressed within two dynamical models based on the macroscopic-microscopic [5] and self-consistent microscopic [6] approaches.

This paper is devoted to the analysis of ratios $\langle N_{L,H}\rangle/Z_{L,H}$ in the primary fission fragments (prior to the neutron evaporation stage) in the correlation with other observables for induced fission of ^{238}U, ^{240}Pu, ^{244}Cm, and ^{250}Cf. For the same fissioning nuclei, there are experimental data, for example, the charge and mass, total kinetic energy (TKE) distributions of fission fragments, and the average number of neutrons emitted from a fission fragment with mass number A_i [the index i designates the light (L) or heavy (H) fragment] [1,2,7–10].

To describe the ratios $\langle N_{L,H}\rangle/Z_{L,H}$ and other fission observables, we employ an improved scission-point model [11–14], where the scission configurations are dinuclear systems (DNS) with two touching individual nuclei (fragments). The improved scission-point fission model is able to consistently and reliably describe several experimental observables in spontaneous and induced fission [11–14].

II. MODEL

In the DNS, the two nuclei interact through the nuclear and Coulomb forces. The resulting nucleus-nucleus interaction potential $V(R)$, which is a function of their relative distance R between nuclei, exhibits a pocket at $R = R_m$ in which the system is trapped for a sufficiently long time such that it reaches statistical equilibrium. Thus, the model assumes that the fission observables are mainly established at the scission configurations. The most important step of this model is the calculation of the potential energy of the DNS as a function of charge Z_i, mass A_i, deformations β_i (the ratios between the major and minor semiaxes of the fragments) of the two fragments, and internuclear distance R between them [11–14]. The potential energy

$$U(Z_i, A_i, \beta_i, E^*) = \sum_{i=L,H}\left[U^{\rm surf}(Z_i, A_i, \beta_i, E_i^*) + U^{\rm Coul}(Z_i, A_i, \beta_i, E_i^*) + U^{\rm asym}(Z_i, A_i, E_i^*) + \delta U^{\rm shell}(Z_i, A_i, \beta_i, E_i^*)\right] + V(R_m) \quad (1)$$

of the DNS is the sum of the interaction energy $V(R_m)$ plus the binding energies of both fragments. The value of R_m is related to Z_i, A_i, and β_i. The binding energies consist of the macroscopic liquid-drop energy $U^{\rm LDM}$ plus the microscopic shell-correction term $\delta U^{\rm shell}$, which is obtained with the Strutinsky procedure and the two-center shell model [11–14]. The macroscopic part of the binding energy consists of excitation-energy dependent surface $U^{\rm surf}(E_i^*)$, Coulomb $U^{\rm Coul}(E_i^*)$, and asymmetry $U^{\rm asym}(E_i^*)$ terms. The shell-correction energies also depend on excitation energy E_i^* as $\delta U^{\rm shell}(Z_i, A_i, \beta_i, E_i^*) = \delta U^{\rm shell}(Z_i, A_i, \beta_i, E_i^* = 0) \times \exp[-E_i^*/E_D]$, where $E_D = 18.5$ MeV is the damping parameter. The excitation energy of the DNS is calculated as the excitation energy of the initial nucleus plus the difference between the potential energy of the initial fissioning nucleus and the potential energy of the DNS. Here, the initial fissioning nucleus is assumed to be in its ground-state deformation. The excitation energy of the system is shared between the two nuclei according to their mass numbers. The relative formation and decay probability $w(A_i, Z_i, \beta_i, E^*)$ of the DNS with particular masses, charges, and deformations of the fragments is calculated within the statistical approach as in Refs. [11–14]. Once the $w(A_i, Z_i, \beta_i, E^*)$ are known, a double integration over the two deformations offer the isotopic yields $Y(Z_i, A_i)$. A subsequent summation over the mass (charge) numbers A_i (Z_i) result in the charge (mass) yields $Y(Z_i)$ [$Y(A_i)$].

Since the fragments are more deformed at scission than in the ground state, the relaxation of the deformations to the ground-state deformations occurs after the DNS decay and the energies of deformations (with respect to the ground-state deformations) are transformed into the fragment intrinsic excitation energies. In order to accurately calculate the neutron multiplicities,

$$\langle n\rangle(A_i) = \sum_{Z_i,\nu}\int d\beta_L\int d\beta_H\,\nu P_\nu(A_i, Z_i, \beta_i, E^*)w(A_i, Z_i, \beta_i, E^*),$$

$$P_\nu = \sum_{x=1}^{\nu}\int_0^{\epsilon^*} d\epsilon_L^* P_C(\epsilon_L^*)P_{xn}(\epsilon_L^*)P_{(\nu-x)n}(\epsilon^*-\epsilon_L^*), \qquad (2)$$

we must take into account the fluctuation of the excitation energy between light and heavy fragments using the microcanonical distribution $P_C(\epsilon_L^*) \sim \rho_L(\epsilon_L^*)\rho_H(\epsilon^*-\epsilon_L^*)$ (where ρ_i is the Fermi-gas level density in fragment i) of energy partitioned between two fragments of the DNS and the Jackson formula [15]

$$P_{xn}(\epsilon_i^*) = P(x) - P(x+1),$$

$$P(x) = 1 - e^{-\Delta_x}\left(1 + \sum_{k=1}^{2x-3}\frac{(\Delta_x)^k}{k!}\right), \qquad (3)$$

for the probability of evaporation of exactly x neutrons from the excited fragment i with excitation energy ϵ_i^* (the sum of the fragment deformation energy with respect to its ground state and the fragment intrinsic excitation energy at scission point) [16]. In Eq. (3), $\Delta_x = (\epsilon_i^* - \sum_{k=1}^{x} B_k^{(i)})/T_i$, where $B_k^{(i)}$ is the experimental neutron binding energy at the kth evaporation step and $T_i = (\epsilon_i^*/a_i)^{1/2}$ is the temperature. Here the quantities $P(x)$ and $P(x+1)$ are the probabilities of emission of at least x and $x+1$ neutrons, respectively. It is clear that $P(x=1) = 1$ at $\epsilon_i^* > B_1^{(i)}$.

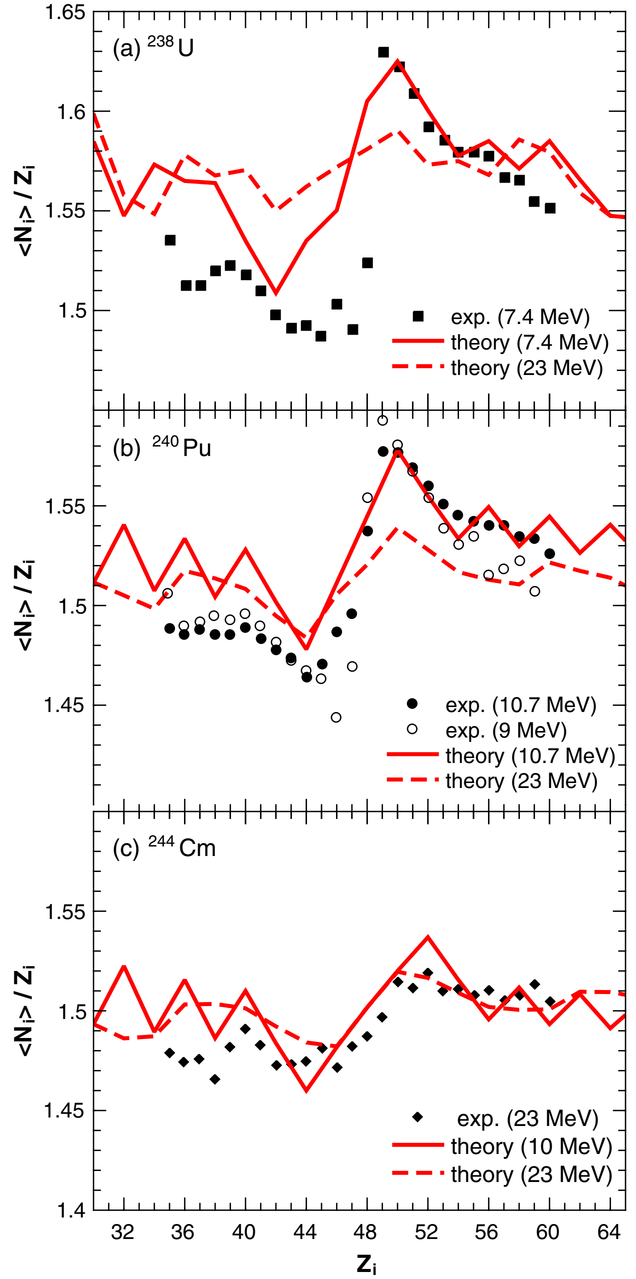

FIG. 1. Calculated $\langle N_i\rangle/Z_i$ ratio for primary fission fragments as a function of Z_i (lines) for ^{238}U (a) at excitation energies 7.4 (solid line) and 23 (dashed line) MeV, ^{240}Pu (b) at excitation energies 10.7 (solid line) and 23 (dashed line) MeV, and ^{244}Cm (c) at excitation energies 10 (solid line) and 23 (dashed line) MeV. The available experimental data are taken from Ref. [2] (closed symbols) and [1] (open symbols). The excitation energy E^* of the fissioning nucleus is presented in parentheses.

III. RESULTS OF CALCULATIONS

In Fig. 1, the theoretical neutron-excess ratios $\langle N_i\rangle/Z_i$ as a function of the fission-fragment charge number Z_i are

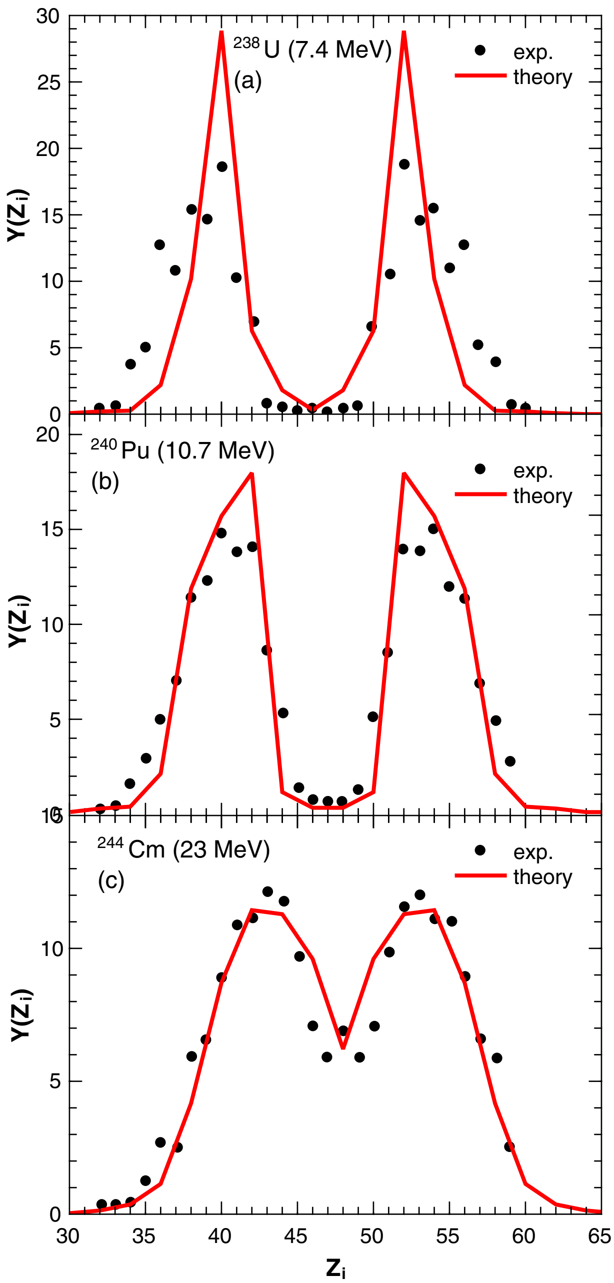

FIG. 2. Calculated charge distributions (solid lines) resulting from the fission of (a) ^{238}U($E^* = 7.4$ MeV), (b) ^{240}Pu($E^* = 10.7$ MeV), and (c) ^{244}Cm($E^* = 23$ MeV) compared with the experimental data (symbols) [2].

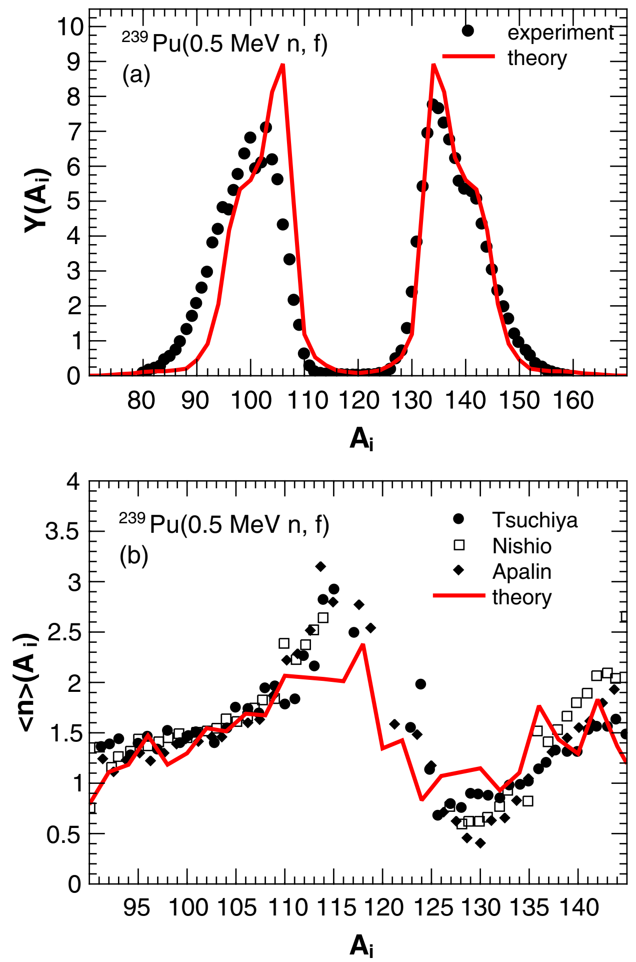

FIG. 3. Calculated (solid lines) (a) primary mass distribution and (b) average number of neutrons emitted by one of the fragments vs the fragment mass number resulting from the 0.5 MeV neutron-induced fission of ^{239}Pu($E^* = 7.4$ MeV). The experimental data (symbols) are taken from Refs. [7–10].

compared with the experimental data [1,2] for the fission of nuclei ^{238}U, ^{240}Pu, and ^{244}Cm. For the same fissioning nuclei, the theoretical and experimental [2,7–10] charge $Y(Z_i)$ and mass $Y(A_i)$ distributions of fission fragments, and the average number $\langle n\rangle(A_i)$ of neutrons emitted from fission fragment with mass number A_i are shown in Figs. 2 and 3. As seen, the experimental data are well described, which demonstrates the capabilities of the model. The position of the maximum of calculated mass distribution of light fragments in Fig. 3(a) is shifted towards the experimental points if neutron emission from the primary fragments is taken into account according to Fig. 3(b). The charge distributions in Fig. 2 are not affected by the neutron emission.

In Fig. 1, the calculated neutron-excess ratio $\langle N_i\rangle/Z_i$ for primary fragments strongly depends on Z_i, exhibiting a structure, which relates to the shell structure of fragments. In the case of fissioning ^{238}U at excitation energy$E^* = 7.4$ MeV [Fig. 1(a)], the minimum located at $Z_L = 32$ is related to the closed shell $N_L = 50$, as the minimum of the potential energy surface (PES) in the charge-mass coordinates comes from the configuration ^{82}Ge + ^{156}Nd. This minimum is related to the maximum of $\langle N_i\rangle/Z_i$ at $Z_H = 60$. At $Z_L = 38$ the neutron shell $N_H = 82$ starts to influence. In this case, the most likely configuration is ^{98}Sr + ^{140}Xe, however, the configurations ^{102}Sr + ^{136}Xe and ^{100}Sr + ^{138}Xe with $N_H = 82$ and $N_H = 84$, respectively, exhibit minima, which are very close in energy, to the minimum corresponding to the ^{98}Sr + ^{140}Xe fragmentation. The same can be noted for the fragmentations ^{A_L}Zr+^{A_H}Te: the minimum of the PES is supplied by the fragmentations ^{102}Zr + ^{136}Te, ^{104}Zr + ^{134}Te, and ^{106}Zr + ^{132}Te with close potential energies (within ≈0.3 MeV). As the atomic number

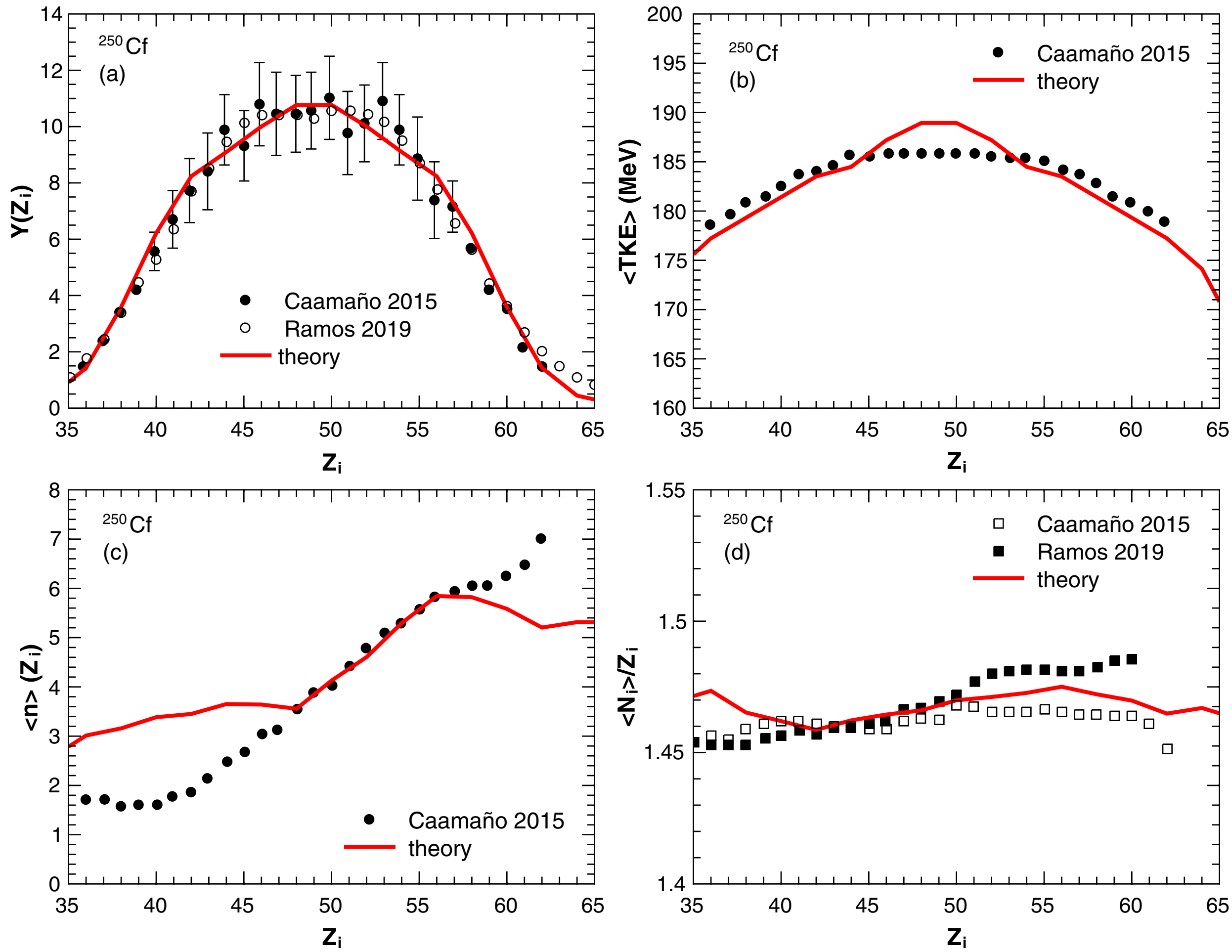

FIG. 4. (a), (b) Calculated (lines) and experimental (symbols) charge and TKE distributions as a function of the charge number of one of the fragments resulting from the fission of ^{250}Cf at an excitation energy of 46 MeV. (c) shows the average number of neutrons emitted from one fragment and (d) shows the neutron-excess ratio $< N_i > /Z_i$, both as a function of the charge number of the light fragment. Solid lines and symbols are theoretical calculations and experimental data of Refs. [1,2], respectively.

of light fragment increases, the heavy fragment becomes double magic. Thus, the ^{106}Mo + ^{132}Sn configuration becomes likely. The shell effects in the heavy fragment hinder a large neutron excess in the light fragment, resulting in the sawtooth structure in Fig. 1. Note that the closed shell $N_H = 82$ is responsible for the decrease of the theoretical $\langle N_i \rangle /Z_i$ in the intervals $Z_H = 50$–54 and $Z_L = 38$–42. In this case the magic neutron number $N_H = 82$ in the heavy fragment tries to keep the neutron number of light fragment.

In the case of fissioning ^{240}Pu at $E^* = 10.7$ MeV [Fig. 1(b)], the average neutron excess of primary fragments has a similar structure as in the case of ^{238}U ($E^* = 7.4$ MeV). The maximum obtained at $Z_L = 32$ and the minimum observed at $Z_L = 34$ are explained by the magic shell $N_L = 50$ of the light fragment in the fragmentations ^{82}Ge + ^{158}Sm and ^{84}Se + ^{156}Nd. The effect of the $N_H = 82$ shell is seen in the configurations ^{102}Zr + ^{138}Xe and ^{104}Zr + ^{136}Xe, which exhibit minima on the PES with close energies. The influence of this neutron shell is also seen in the ^{106}Mo + ^{134}Te configuration. In the same manner as in the ^{238}U case, the combined effect of both $Z_H = 50$ and $N_H = 82$ shells create the sawtooth feature shown in Fig. 1. In the minimum of $\langle N_i \rangle /Z_i$ at $Z_L = 44$, the most probable DNS are ^{108}Ru + ^{132}Sn and ^{110}Ru + ^{130}Sn. Note that the structure in $\langle N_i \rangle /Z_i$ (Fig. 1) appears in the calculations for primary fragments. Therefore, the neutron emission from the fission fragments is not the reason for this structure. As follows from Figs. 3(b) and 1(b), the neutron emission would deepen the minimum of $\langle N_i \rangle /Z_i$ at $Z_i = 44$, i.e., highlight the sawtooth structure.

In the case of fissioning ^{244}Cm at excitation energy of 23 MeV [Fig. 1(c)], a similar analysis is performed for fissioning nuclei ^{238}U ($E^* = 7.4$ MeV) and ^{240}Pu ($E^* = 10.7$ MeV). In this case the excitation energy is much higher, so the shell effects are dampened and, as a result, the neutron-excess ratio $\langle N_i \rangle /Z_i$ does not exhibit such a strong dependence on the charge number of the fission fragment. In Fig. 1(a), 1(b) the predicted neutron-excess ratios of the fission fragments in the cases of fissioning nuclei ^{238}U and ^{240}Pu at an initial excitation energy of 23 MeV are also presented. As seen, the sawtooth character of the $\langle N_i \rangle /Z_i$ is less pronounced.

Figure 4(a), 4(b) shows the calculated charge and TKE distributions for the fission of ^{250}Cf at an excitation energy of 46 MeV. In Fig. 4(c), the average number of neutrons emitted by a fragment with charge number Z_i is compared with experimental data of Ref. [1]. One striking feature of Fig. 4(c) compared to Fig. 3(b) is the fact that in the case of high-energy fission of ^{250}Cf the $\langle n\rangle$ distribution does not have the sawtooth shape of Pu, but rather a steady increase in neutron multiplicity as the heavier fragment receives more and more excitation energy in proportion to its mass number. In Fig. 4(d), the neutron excess $\langle N_i\rangle/Z_i$ of one of the fragments is presented. In this case, the values are fairly constant, which agrees with the experimental data [1,2]. The explanation for this is the same as discussed earlier, namely, the melting of shell effects at high excitation energy.

Note that for the corresponding nuclei, the ratios $\langle N_i\rangle/Z_i$ for primary fragments in Refs. [11–14] coincide with those calculated here. Since neutron multiplicities are calculated here using the Jackson formula [15], they are about 0.6 units less than the corresponding values in Refs. [11–14], where the number of evaporated neutrons is continuous variable in contrast to that in the present model.

Ratios $\langle N_i\rangle/Z_i$ of primary fission fragments resulting from the fission of ^{240}Pu at $E^* = 6.54$, 10, and 20 MeV and $E^* = 7.5$, 10.5, 12.5, and 16.5 MeV are analyzed within the macroscopic-microscopic [5] and self-consistent microscopic [6] approaches, respectively. Our conclusions about the neutron-excess in the fission fragments are consistent with the conclusions of Refs. [5,6], namely, that with increasing excitation energy, fragments tend to have the same neutron-to-proton ratios as in a fissioning compound nucleus. However, it is worth noting that in our case, the transition to a constant $\langle N_i\rangle/Z_i$ is slower with increasing excitation energy, than in the cases presented in Refs. [5,6].

IV. CONCLUSIONS

In conclusion, our study of low-energy fission shows that the neutron-excess ratio $\langle N_i\rangle/Z_i$ of fission fragments has a strong dependence on the fragment charge number Z_i, exhibiting a well-defined sawtooth structure, which is the direct result of the interplay between the neutron and proton shell closures. For example, if the neutron number in one of the fission fragments is close to the magic one, there is interval of Z_i where N_i is almost unchangeable. In this case the neutron-excess ratio $\langle N_i\rangle/Z_i$ decreases with increasing Z_i. Furthermore, this structure is a property of the primary fragments and not a consequence of the neutron emission from the fragments after postseparation. As such, one can not imply that the $\langle N_i\rangle/Z_i$ ratio of the initial fissioning compound nucleus is preserved in the primary fission fragments, but rather this assumption should be made only for high excitation energies, where the shell effects are considerably reduced.

ACKNOWLEDGMENTS

This work was supported by Ministry of Science and Higher Education of the Russian Federation (Contract No. 075-10-2020-117). The work of H.P. was also supported by a grant of the Romanian Ministry of Education and Research, CNCS - UEFISCDI, Project No. PN-III-P1-1.1-PD-2019-0304, within PNCDI III.

[1] M. Caamaño, F. Farget, O. Delaune, K.-H. Schmidt, C. Schmitt, L. Audouin, C.-O. Bacri, J. Benlliure, E. Casarejos, X. Derkx, B. Fernández-Domínguez, L. Gaudefroy, C. Golabek, B. Jurado, A. Lemasson, D. Ramos, C. Rodríguez-Tajes, T. Roger, and A. Shrivastava, Phys. Rev. C **92**, 034606 (2015).

[2] D. Ramos, M. Caamaño, F. Farget, C. Rodríguez-Tajes, L. Audouin, J. Benlliure, E. Casarejos, E. Clement, D. Cortina, O. Delaune, X. Derkx, A. Dijon, D. Doré, B. Fernández-Domínguez, G. de France, A. Heinz, B. Jacquot, C. Paradela, M. Rejmund, T. Roger *et al.*, Phys. Rev. C **99**, 024615 (2019).

[3] D. Ramos, M. Caamaño, A. Lemasson, M. Rejmund, H. Alvarez-Pol, L. Audouin, J. D. Frankland, B. Fernádez-Domínguez, E. Galiana-Baldó, J. Piot, C. Schmitt, D. Ackermann, S. Biswas, E. Clement, D. Durand, F. Farget, M. O. Fregeau, D. Galaviz, A. Heinz, A. Henriques *et al.*, Phys. Rev. C **101**, 034609 (2020).

[4] J.-F. Martin, J. Taïeb, G. Boutoux, A. Chatillon, T. Gorbinet, E. Pellereau, L. Audouin, A. Heinz, H. Alvarez-Pol, Y. Ayyad, G. Bélier, J. Benlliure, M. Caamaño, E. Casarejos, D. Cortina-Gil, A. Ebran, F. Farget, B. Fernández-Domínguez, L. Grente, H. T. Johansson, B. Jurado *et al.*, Phys. Rev. C **104**, 044602 (2021).

[5] C. Schmitt and P. Moller, Phys. Lett. B **812**, 136017 (2021).

[6] M. Verriere, N. Schunck, and D. Regnier, Phys. Rev. C **103**, 054602 (2021).

[7] K. Nishio, Y. Nakagome, I. Kanno, and I. Kimura, J. Nucl. Sci. Technol. **32**, 404 (1995).

[8] T. R. England and B. F. Rider, LANL Report No. LA-UR-94-3106, 1994.

[9] C. Tsuchiya, Y. Nakagome, H. Yamana, H. Moriyama, K. Nishio, I. Kanno, K. Shin, and I. Kimura, J. Nucl. Sci. Technol. **37**, 941 (2000).

[10] V. F. Apalin, Yu. N. Gritsyuk, I. E. Kutikov, V. I. Lebedev, and L. A. Mikaelian, Nucl. Phys. A **71**, 553 (1965).

[11] H. Paşca, A. V. Andreev, G. G. Adamian, and N. V. Antonenko, Phys. Lett. B **760**, 800 (2016); Phys. Rev. C **94**, 064614 (2016).

[12] H. Paşca, A. V. Andreev, G. G. Adamian, and N. V. Antonenko, Phys. Rev. C **97**, 034621 (2018).

[13] H. Paşca, A. V. Andreev, G. G. Adamian, and N. V. Antonenko, Nucl. Phys. A **969**, 226 (2018).

[14] H. Paşca, A. V. Andreev, G. G. Adamian, and N. V. Antonenko, Phys. Rev. C **101**, 064604 (2020); **104**, 014604 (2021).

[15] R. Vandenbosch and J. R. Huizenga, *Nuclei Fission* (Academic, New York, 1973).

[16] H. Paşca, A. V. Andreev, G. G. Adamian, and N. V. Antonenko (unpublished).